DRIFT MEASUREMENTS OF THE *E*-LAYER

BY

L. HARANG and K. PEDERSEN

Norwegian Defence Research Establishment

(Manuscript received September 14th 1956)

SUMMARY

The drift of the diffraction pattern on the ground due to *E*-layer reflections has been recorded at Kjeller (φ = 59° 58′ N. λ = 10° 06′ E) on 2 Mc/s during the period June 1953 to Sept. 1955.

Three receiving points were put up and the amplitudes of the *E*-echoes were recorded (Mitra-method). The time-shifts between the maxima in the fading curves were recorded automatically by means of a Phillips recorder or, optically by a three-beam oscillograph.

The diurnal values of the E—W and N—S components of the drift in m/s have been given for each month through curves. For the seasons winter, spring, summer and autumn the mean values are given in tables.

The seasonal and annual curves have been analyzed and the mean values compared with the results from similar recordings at Cambrigde, Washington and Ottawa.

There is a constant term indicating a prevailing drift towards SW in the winter and towards *NE* in the summer. There is a solar 12-hours term appearing during all seasons of the year. The mean annual values of phase and amplitude of this term at Kjeller are very similar to the corresponding term at Cambridge

The summer values have been analysed for a lunar term, and a small but doubtful component has appeared.

A 100—160 km height gate was used to isolate the *E*-echoes. During *daytime* there seems to be no systematic change in the wind direction on days with *Es* or normal *E*. At sunset when the electron density of the normal *E*-layer is too low for reflecting the test frequency 2 Mc/s, there is a sudden change in the direction of the E-W component. The *Es*-layer recorded after sunset and during the night has a strong Western component.

On account of the gate width it is not possible to decide whether this is a height effect. Another explanation is that the diffraction pattern during night time is not isotropic, but has a preferred orientation in N-S direction. This will simulate a strong increase in the E—W component of the drift.

The probability distribution of the timeshifts has been studied in the simple cases of drift along one of the main bases or along a diagonal. It is pointed out that the probability distribution along the N—S direction is systematically narrower than along the E—W direction. Examples of very narrow probability distributions in N—S direction at night are given The conclusion reached is that there seems to he a preferred orientation in N—S direction of the lines of maxima during day time, which during night time may be predominant.

The drift was measured during the solar eclipse on June 30th 1954 at Kjeller, where the degree of the eclipse was 99 %. The eclipse had a pronounced effect on the drift direction, due to the complex nature of the *E*-layer on this day, the *E*-layer consisting of *E* + *Es*. During the eclipse the critical frequency of the *E*-layer decreased beyond 2 Mc/s and reflection was obtained only from *Es*. There was a reversal of the drift direction during this period.

1.0 INTRODUCTION

There are a number of phenomena appearing in the upper atmosphere which indicate the existence of winds in the heights of 80—120 km. Observations of the luminous nightclouds, luminous trails of meteors lying in the sunlit atmosphere, and the drift of certain auroral forms, indicate a horizontal movement of the air masses with speeds up to about 100 m/s. However, all

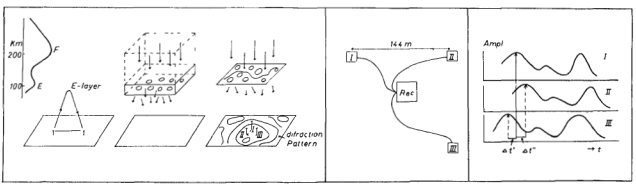

Fig. 1. Method for measuring the drift of the diffraction pattern on the ground.

of these classes of observations can only be made occasionally, and they do not allow a systematic study of the wind-systems during the day and the year. In this respect the radio methods, which are based on the study of the drift of the diffraction pattern on the ground, represent a new and most valuable approch to the question of movements, as this method permits continous observations to be made over a longer period.

The older methods have, however, certain merits and have demonstrated a number of facts which have to be considered when the results from the radio methods are being discussed. The parallactic photos of night-clouds by Störmer[1] showed that these were lying at a height of 81 km, and had a mean speed of drift of 44—55 m/s towards SSW (photographed) in the evening over Southern Norway in July 1932. In addition to the main drift of the clouds the photos showed a number of finer details which demonstrated the existence of «waves» in the cloud of a magnetude of 7 to 9 km. Further, the succesive photos demonstrated a continous change and deformation of the clouds indicating the presence of large scale turbulence and eddies in this level of height.

The succesive photos of the *meteor trains* indicate a rapid change, and even reversals, in the wind direction *with height*. This effect has been studied quantitatively by Liller and Whipple[2] from photos of meteorite trains obtained using the super-Schmidt camera of the Harvard Observatory. From an analysis of five trains they conclude that the wind directions may show no correlation when the height intervals are 5 km or greater. In some cases they even find an indication of a reversal with height. The height of the trains measured were in the interval 81—113 km.

When attempting to interprete the drift of the diffraction pattern on the ground as an indication of an horizontal drift of the ionosphere at a certain level, we have therefore to consider the effects already stated from other fields of research, *a.* the existence of large scale eddies and waves, and *b.* the rapid change in wind directions with height.

The method for measuring the drift of the ionozed layers first introduced by Mitra[3] was used, see fig. 1.

When using a pulsed transmitter on 2 Mc/s the normal *E*-layer will during the day reflect the wave as an *E*-echo. Due to inhomogenities in the *E*-layer, the transmitted plane wave will, when reflected, be broken up into an angular spectrum of components. On the ground the field-strength of the angular components will add together and we obtain a field-strength-landscape of varying topography depending on the amplitudes and phases of the angular components. The *drift* of this diffraction pattern on the ground can be studied by recording the amplitudes of the fading *E*-echoes at three points. The velocity of drift of the pattern will be *twice* the drift of the ionosphere.

We have here made the following assumptions:

a. the shape of the diffraction pattern is constant in form and isotropic during the time of measurement, and
b. the three receiving points are lying within the same «topography» of the field-strength landscape.

Usually these two assumptions are only partly fulfilled and in some cases even far from being fulfilled.

2.0 INSTRUMENTAL EQUIMENTS

Three *antennae* were placed in a triangle with directions N—S and E—W. The antenna placed at the right angle was used as reference antenna, and the relative displacements in time of the maxima of the fadings recorded from the two other antennae were measured. The antennae were sited on flat ground west of the main laboratory building of the institute. The site was not ideal due to the vicinity of various buildings and we had to change the position of the antenna-net several times because of the erection of new buildings. During July—Oct. 1955 we had the opportunity of erecting the antennae on the open ground of the Kjeller airfield, which offered an ideal site for these recordings.

In table 1 the length of the base lines during different periods are given.

The first antennae-net consisted of three receiving points. The fourth net, erected on the Kjeller airfield, had five receiving points and we could use alternatively 130 and 260 m bases.

Only open antennas were used. Open *L*-antennas were used at the outer receiving points in the two first nets, the central antenna being a delta-antenna which also was used for pulse transmission. An R—T switch was used in order to operate the transmitter and the receiver on the same antenna.

In the two last nets frame antennae were used at all three receiving points. Frames 15×3 m^2 with their planes vertical and in N-S directions were erected at an height of 5 m above the ground and tuned to 2 Mc/s. Each receiving point was connected by a 300 ohm feeder to one of three separate receivers in the recording hut. The frames seemed to give a better signal/noise ratio than the open *L*-antennas.

The *transmitter* used was a copy of a pulse-transmitter developed by Lied[4] for absorption studies at Kjeller, and consisted of a pulsed oscillator and a broadband power amplifier. The peak-power of the pulses was about 8 kW and the usual pulse-length was 150μ sec. The transmitter was coupled to the antenna through a 600 ohm feeder, the antenna being of the delta-type commonly used in broad-band ionospheric work,

The *receivers*, were of a conventional echo study type and consisted of two stages HF amplification mixer and two stages IF at 450 kc/s. The band-width was 30 kc/s. Following the IF stages an infinite impedance detector is used and the signal is fed through a cathode follower into the LF-panels for further analysis. A pulse of suitable width and phase from a special pulsegenerator is applied to the gated amplifier in order to isolate the *E*-echoes. The echoes are further amplified and displayed as a continous curve through a peak-voltmeter of suitable time-constant.

Special attention had to be paid to the volume control of the receivers. During a period of recording which could last for more than half an hour, the mean field strength of the *E*-echoes could vary considerably. For analysis of the fading record it is however necessary, that the mean amplitudes of the fading *E*-echoes in the output are of the same magnitude during the time of registration and an AVC-system had therefore to be used. The time constant of the AVC voltage was about 2 minutes and was applied to the suppressor-grids of the two HF-and the two IF-valves.

Table 1.

	E—W	N—S	Period
Site at the	76 m	137 m	Jun. 1953—Aug. 1953
Institute	78 -	79 -	Aug. 1953—Sep. 1954
	143 -	146 -	Oct. 1954—Jul 1955.
Kjeller Airfield ..	130 and 260 m	130 and 260 m	Jul. 1955—Oct. 1955

3.0 THE METHODS OF RECORDING THE AMPLITUDES OF THE FADING E-ECHOES

a) *Optical Method.*

The echo patterns from the three receivers could be displayed simultaneously on the screen of a three-beam oscillograph, and by connecting a gating circuit to the intensity modulation of the CRT, only echoes from the *E*-region in the height interval of about 100—160 km were shown on the screen. The three displays were placed side by side on the screen with their echo amplitudes shown horizontally, and the amplitude variations were recorded on a slowly moving photographic paper. During the first year all registrations were made using this technique, and usually one three-minute record was taken each half an hour.

This method of recording each fading curve separately, gives the most complete information about the character of the fading curve and the properties of the diffraction pattern. In fig. 2 is shown four record strips which demonstrate different properties of the diffraction pattern.

a shows smooth, regular and coherent fading at all three points, a pattern of constant form is drifting. On *b* the fadings are still regular, but there is some lack of coherence between the fadings at the three receiving points. On *c* we have almost constant field-strength at all three points, an *E*s-layer of almost mirror-like character is present. *d* is a record taken during a geomagnetic storm, with very rapid fading down to a period of 1 c/s. Two effects are present here. There is a great increase in drift velocity, (corresponding to small relative displacements of the maxima) and only slight coherence between the fadings, indicating that the «scale» of the diffraction pattern has decreased.

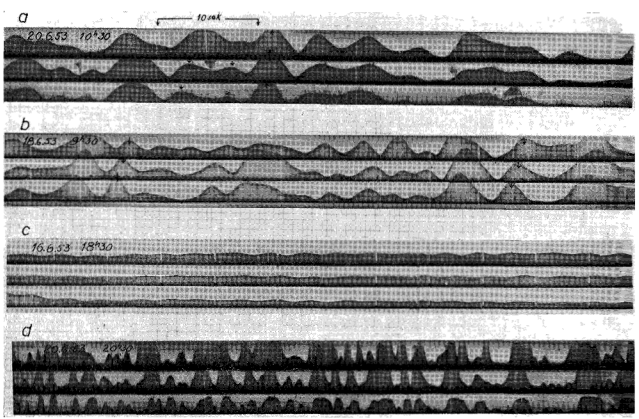

Fig. 2. *a*, *b*, *c* and *d*. Different types of fading curves.

The great variability in the winds indicated however, that this short time interval for recording must be considered as insufficient for giving representative values. The great consumption of paper and the labour involved in reducing the records made an extension of the recording time unsuitable. A fading recorder according to the principle of Phillips was therefore built.

b) *Electrical Method.*

The purpose of this method was to avoid the simultaneous recording of three separate and complete fading curves. For determination of the wind we are principally interested in measuring the mean relative displacement in time between the fading-maxima of the three curves. This process can be done electronically by means of the Phillips recorder. The instrument is described in the Thesis of G. J. Phillips (Cambridge 1951) and Dr. Phillips has most kindly circulated a short description of this recorder and thus made it possible in short time to build a recorder similar to the type which has been in use in Cambridge. Phillips has given the following short description of the purpose of the recorder. «The circuit is designed to accept two D. C. potentials varying in proportion to the amplitude of an ionospheric echo at the two receiving points on the ground. Every time both inputs drop to a minimum and increase again, a change is produced which is proportional to the time between the occurrance of the two corresponding minima in each channel, and which is fed to the output terminals with a polarity depending in which channel has its minimum ahead of the other. These charges are fed to a centrezero pen recorder so that a «spike» is produced corresponding to each charge, this forms a continous record of the amplitude and sense of the time-delay between the two wave-forms as estimated from the time of occurance of the minima». The type of record produced is shown in fig. 3.

In order to calibrate the records a special LF-oscillator had to be built. It consisted of a generator which could give two voltages of the same

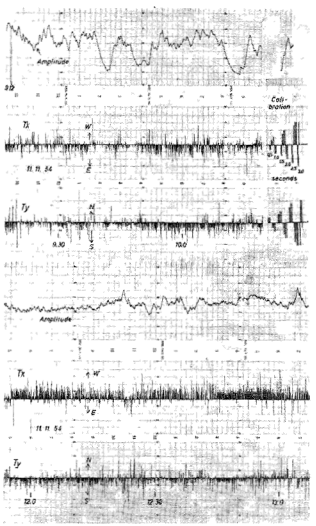

Fig. 3 Strips of wind-records taken according to the Phillips system. The upper strip shows a record with considerable variations in the mean fading amplitude, the lower strip shows a record with small variations in the mean fading amplitude.

amplitudes, but with varying phases relative to each other. These two voltages thus simulated two fadings with varying displacements of amplitudes relative to each other. The two voltages were applied to be Phillips recorder and the «spikes» were recorded for time-shifts of 0,5, 1,0, 1,5, 2,0, 2,5 and 3,0 sec of the waves relative to each other. A frequency corresponding to a period of a fading of T = 8 sec was used.

4.0 DISCUSSION OF THE DIURNAL RECORDS

Observations were made over the period Jun. 1953 to Sept. 1955. During the period June 1953 to May 1954 the optical method was used for recording, a record of the fadings during a period of three minutes being taken automatically each hour. In June 1954 we changed over to the Phillips recorder and a record of the fadings during a period of ten minutes was taken automatically each hour, during some periods during each half an hour.

The first step will be to use the daily records to extract mean monthly and seasonal values of the drift of the diffraction pattern along the ground.

The principle of the analysis of fading records obtained at three receiving points in order to determine the drift has been given by Mitra[3] Briggs, Phillips and Shinn[5], Briggs and Phillips[6] Phillips[7] and Ratcliffe[8], and in the following the same symbols will be used which have been introduced in the papers mentioned.

The receiving points were located at the corners of a triangle whose vertex angle was near 90°. During the last period of recording the spacings were nearly equal, respectively 143 and 146 m. The frequency used was near 2.0 Mc/s, for practi-

Table 2. Drift velocities

	0	1	2	3	4	5	6	7	8	9	10
1954 Summer	0	5 N	10 S	9 S	7 N	33 N	50 N	66 N	67 N	62 N	47 N
1955 —	12 N	15 N	10 N	5 S	5 S	4 N	10 N	17 N	3 N	10 S	26 S
Mean	6 N	10 N	0	7 S	1 N	19 N	30 N	42 N	35 N	26 N	10 N
1953 Autumn	(0)	(0	(0)	(0)	10 N	0	20 S	44 S	52 S	60 S	50 S
1954 —	(70 N)	(70 N)	(70 N)	66 N	60 N	50 N	50 N	50 N	55 N	50 N	50 N
Mean	35 N	35 N	35 N	33 N	35 N	25 N	15 N	3 N	2 N	5 S	0
1953—54 Winter	30 S	33 S	30 S	20 S	20 S	17 S	10 S	10 S	27 S	40 S	47 S
1954—55 —	5 N	7 N	12 N	(0)	(12 S)	(25 S)	(35 S)	(50 S)	65 S	60 S	60 S
Mean	13 S	13 S	9 S	10 S	16 S	21 S	23 S	30 S	46 S	50 S	53 S
1954 Spring	(0)	6 S	12 S	12 S	0	20 N	30 N	40 N	46 N	40 N	36 N
1955 —	(50 N)	47 N	47 N	40 N	15 N	0	12 S	17 S	22 S	25 S	30 S
Mean	25 N	22 N	18 N	14 N	8 N	10 N	9 N	12 N	12 N	8 N	3 N
Mean 53—54	8 S	9 S	13 S	10 S	1 S	9 N	15 N	13 N	9 N	1 N	4 S
Mean 54—55	34 N	35 N	35 N	25 N	15 N	7 N	5 N	0	7 S	11 S	17 S
Total Mean	13 N	13 N	11 N	8 N	7 N	8 N	10 N	7 N	1 N	5 S	11 S

E — W

1954 Summer	52 W	62 W	58 W	42 W	8 W	5 E	57	73 E	75 E	75 E	83 E
1955 —	75 W	72 W	72 W	50 W	40 W	40 E	60 E	65 E	72 E	70 E	62 E
Mean	64 W	67 W	65 W	46 W	24 W	23 E	59 E	69 E	73 E	73 E	73 E
1953 Autumn	(0)	(0)	(0)	(0)	(0)	0	0	5 W	10 W	20 W	30 W
1954 —	80 W	70 W	50 W	10 E	50 E	50 E	50 E	50 E	40 E	35 E	10 E
Mean	40 W	35 W	25 W	5 E	25 E	25 E	25 E	22 E	15 E	7 E	10 W
1953—54 Winter	52 W	57 W	60 W	50 W	36 W	20 W	2 E	25 E	45 E	23 E	3 W
1954—55 —	107 W	120 W	127 W	(100W)	(90 W)	(80 W)	(70 W)	(60 W)	(70 W)	(80 W)	93 W
Mean	80 W	88 W	94 W	75 W	63 W	50 W	34 W	18 W	12 W	28 W	48 W
1954 Spring	0	10 W	24 W	30 W	36 W	24 W	0	20 E	30 E	30 E	28 E
1955 —	(80 W)	77 W	72 W	55 W	32 W	12 W	16 E	27 E	35 E	30 E	25 W
Mean	40 W	44 W	48 W	43 W	34 W	18 W	8 E	24 E	33 E	30 E	2 E
Mean 53—54	26 W	32 W	35 W	31 W	20 W	10 W	15 E	28 E	35 E	27 E	20 E
Mean 54—55	86 W	85 W	80 W	49 W	28 W	1 W	14 E	21 E	19 E	14 E	12 W
Total mean	56 W	59 W	58 W	40 W	24 W	6 W	15 E	25 E	27 E	21 E	4 E

cal reasons we had to change this between the limits 1.88 to 2.22 Mc/s. The noise level of the site was fairly high and we did usually not obtain reliable records on days with high absorption. From the records taken only 20—40 % of the hours recorded during the day gave reliable hourly values which can be used in the discussion. During the night the normal *E*-echoes were not present, and one has to use the *Es*-echoes occasionally occuring. The number of successful night values is therefore considerably less than the number of day values, and further, the height of the reflecting layer during the night will be less defined than during the day. During the day we can usually assume normal *E*-echoes or *Es*-echoes from the usual height of 110 km. During the night all types of layers appearing within the width of the gate, which extended from 100 km to about 160 km would be recorded.

From the records the «mean time of displacements», $\overline{T}_x$ and $\overline{T}_y$ (in E—W and N—S directions), can be taken out during spaced time of recordings. Following Ratcliffe's discussion[8] we have the following equations for determining the speed of wind, V, and the direction Φ:

$$(\overline{T}_x)^2 + (\overline{T}_y)^2 = a^2/V^2$$

and

$$tg\Phi = \overline{T}_y/\overline{T}_x,\ V_x = V\cos\Phi,\ V_y = V\sin\Phi$$

where a is the spacing of the receivers. We have

in m/s. N—S component.

11	12	13	14	15	16	17	18	19	20	21	22	23	Mean
34 N	6 N	8 N	37 N	57 N	62 N	62 N	57 N	37 E	5 S	38 S	47 S	22 S	23 N
40 S	50 S	20 N	43 N	47 N	45 N	30 N	25 N	10 S	46 S	14 S	18 N	22 N	5 N
4 S	22 S	14 N	40 N	52 N	53 N	46 N	41 N	13 N	26 S	26 S	14 S	0	14 N
26 S	0	30 N	44 N	44 N	36 N	25 N	25 N	24 N	17 N	(10 N)	(15 N)	(0)	1 N
55 N	58 N	58 N	55 N	55 N	65 N	55 N	55 N	60 N	60 N	(65 N)	(75 N)	(75 N)	56 N
14 N	29 N	44 N	50 N	50 N	50 N	40 N	40 N	42 N	39 N	38 N	45 N	38 N	29 N
45 S	40 S	37 S	24 S	3 S	12 N	17 N	15 N	13 N	3 N	2 S	(10 S)	(10 S)	16 S
25 S	7 N	25 N	20 N	37 N	27 N	3 N	17 S	(15 S)	10 S)	(5 S)	(5 S)	(0)	10 S
35 S	17 S	6 S	2 S	17 N	20 N	10 N	1 S	1 S	4 S	4 S	8 S	5 S	13 S
35 N	36 N	36 N	34 N	36 N	42 N	40 N	36 N	30 N	(35 N)	(40 N)	(44 N)	(20 N)	26 N
15 S	0	17 N	45 N	45 N	28 N	0	35 S	50 S	47 S	38 S	10 S	10 N	2 N
10 N	18 N	27 N	40 N	40 N	35 N	20 N	0	5 S	6 S	1 N	17 N	15 N	14 N
1 S	0 N	9 N	23 N	34 N	38 N	35 N	33 N	26 N	14 N	3 N	1 N	3 S	9 N
6 S	4 N	30 N	41 N	46 N	41 N	22 N	9 N	4 S	11 S	2 N	20 N	27 N	15 N
4 S	2 N	20 N	32 N	40 N	40 N	29 N	21 N	11 N	2 N	3 N	11 N	12 N	12 N

component

77 E	57 E	28 E	22 E	52 E	58 E	66 E	68 E	60 E	17 E	22 W	40 W	46 W	22 E
57 E	50 E	45 E	57 E	80 E	82 E	90 E	95 E	87 E	0	67 W	90 W	90 W	22 E
67 E	54 E	37 E	40 E	66 E	70 E	78 E	82 E	73 E	9 E	45 W	65 W	68 W	22 E
38 W	40 W	30 W	0	36 E	48 E	25 E	5 E	(0)	(0)	(0)	(0)	(0)	2 W
5 E	0	15 E	28 E	25 E	20 E	20 E	10 E	(10 W)	(50 W)	(50 W)	(90 W)	(80 W)	2 W
17 W	20 W	7 W	14 E	30 E	36 E	23 E	8E	5 W	25 W	25 W	45 W	40 W	2 W
15 W	35 W	65 W	62 W	48 W	32 W	20 W	15 W	10 W	10 W	22 W	32 W	45 W	25 W
102 W	108 W	108 W	83 W	17 W	47 E	48 E	20 W	35 W	(50 W	(65 W)	(80 W)	(90 W)	69 W
58 W	72 W	87 W	73 W	33 W	7 E	14 E	18 W	23 W	30 W	44 W	56 W	68 W	47 W
16 E	8 E	6 W	6 W	20 E	24 E	24 E	14 E	20 W	48 W	48 W	(0)	(0)	3 W
55 W	79 W	90 W	88 W	20 W	50 E	92 E	76 E	0	5 W	(42 W)	(60 W)	(80 W)	23 W
20 W	36 W	48 W	47 W	0	37 E	56 E	46 E	10 W	27 W	45 W	30 W	40 W	13 W
10 E	3 W	18 W	12 W	15 E	25 E	24 E	18 E	8 E	10 W	23 W	18 W	23 W	2 W
26 W	34 W	35 W	22 W	17 E	51 E	63 E	40 E	11 E	26 W	56 W	80 W	85 W	18 W
8 W	19 W	27 W	17 W	16 E	38 E	44 E	29 E	10 E	18 W	40 W	49 W	54 W	10 W

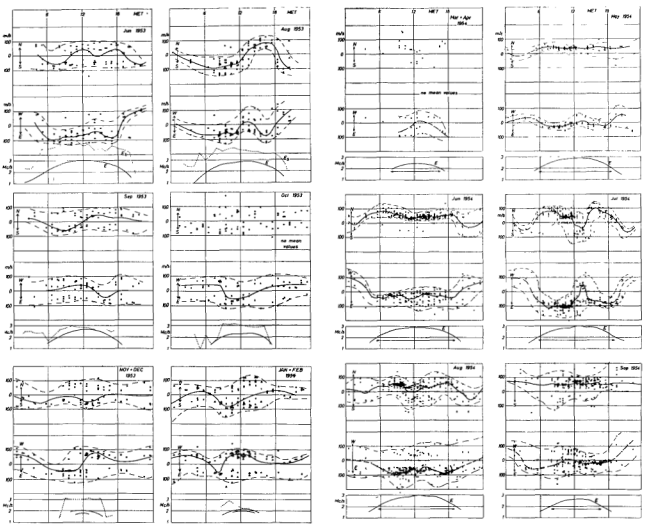

Figur 4 a and b. Hourly values of the drift of the E-layer.

here made the assumption that the diffraction pattern on the ground is isotropic, *i. e.* that the «lines of maximum» appear equally at random in all directions.

In their analysis of the movement of the diffraction pattern Briggs, Phillips and Shinn[5] define the drift velocity along the X-axis, $V_x = V\cos \Phi$, as the velocity with which an observer would have to move along the X-axis in order to reduce the speed of fading as observed by him to a minimum.

In the presentation of the results we shall accept the assumption that the diffraction pattern can be regarded as isotropic. The velocities given are therefore considered as true velocities of the drift of the diffraction pattern. In section 10 effects of anisotropy of the diffraction pattern in the character of the records will be discussed.

In fig. 4 *a*, *b*, *c* and *d* we have given the mean hourly values recorded during each month. The mean monthly curve has been drawn from median values.

The mean monthly value of the critical frequencies of the normal E-layer recorded at Kjeller is also given, indicating the period of the day during which the normal E-echoes have been used for wind recordings. The broken line indicate Es.

In fig. 5 the mean monthly diurnal curves are given. Reliable values are indicated by dots, the crosses indicating values which have been estimated from few and scattered observations occuring usually during the night.

From the curves in fig. 4 is evident that the number of observations, has increased in 1954—55.

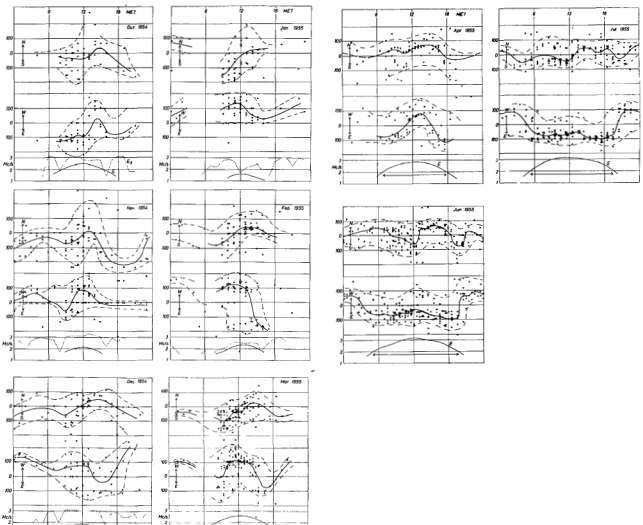

Fig. 4 c and d Hourly values of the drift of the *E*-layer

During the last year it was usually recorded on 2—3 days each week. The accuracy with which a single hourly value can be given is estimated to 20—30 %, and the great scattering of separate readings must therefore be regarded as real. However, with sufficient observations it is evident that a mean diurnal variation characteristic for each season of the year is present.

In table 3 the mean values for each of the four seasons have been given for each of the two years, 1953—54 and 1954—55, and in fig. 6 the diurnal curves for each of the seasons are shown. The values given here are *half values of the drift velocities of the diffraction pattern, and should thus give the values of the assumed E-layer wind.*

Although there are considerable individual differences between the seasonal curves from the two years, the main character of the variation from one year to the next seems to be maintained. Of the four seasons the summer values are by far the more reliable and it is interesting to compare the curves from the two summers 1954 and 1955. The E—W component is almost identical during the two years, but the N—S component shows a systematic displacement towards lower values during the first twelve hours of the day. In this case we should regard this change from one year to the next as real. There is also a slight displacement of about one hour in the position of the maxima in both the E—W and N—S components for 1955 when compared with 1954.

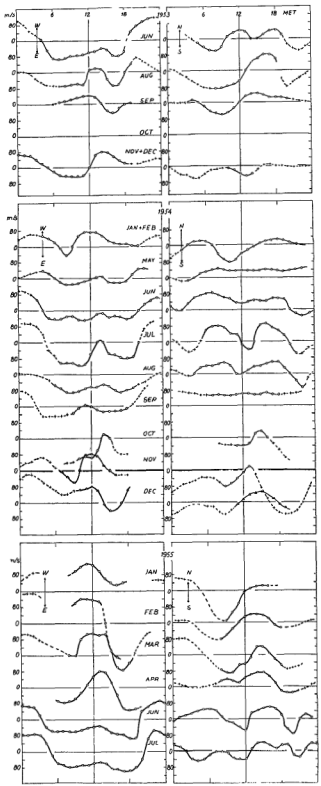

Fig. 5. Mean monthly diurnal curves of the drift of the E-layer. The dots indicate reliable values. the crosses indicate values which have been estimated from few and scattered observations.

A Fourier analysis of the mean seasonal curves for Kjeller gave the following coefficients, containing only the constant term and the 24 and the 12 hours terms:

$$V = a + c_1 (\sin t + \varepsilon_1) + c_2 (\sin 2t + \varepsilon_2).$$

Table 3.

		a	c_1	c_2	ε_1	ε_2	
		m/s	m/s	m/s	°	°	
Summer ...	V_x	21	38.2	— 95	—103	E–W
	V_y	15	15.0	18.2	— 90	— 45	N–S
Autumn ...	V_x	— 3	17.7	23.2	— 72	— 59	E–W
	V_y	31	19.1	12.2	154	11	N–S
Winter.....	V_x	—47	18.3	33.1	—146	—106	E–W
	V_y	14	19.0	14.1	159	— 7	N–S
Spring	V_x	—12	19 5	32.6	— 99	—104	E–W
	V_y	14	5.6	10.8	—104	20	N–S
Mean	V_x	—10.5	30.0	31.4	—100	— 97	E–W
	V_y	11.8	10.1	12.0	—169	— 14	N–S

In these series the negative values designate drift towards respectively W- and S-directions.

In fig. 8 the variation of the components during the seasons are demonstrated through harmonic dials.

The representation of the observed values through a three-terms Fourier series can not be regarded as satisfactory. In fig. 7 the actual observations have been compared with the Fourier-synthesis, and there is an especial difference between the position of the maxima of the assumed 12-hours component and the observed maxima.

As pointed out by Briggs and Spencer[9] this is partly due to the fact that the time for rotation of the 12-hours term actually seems to be less, of about 8—10 hours, and this effect also occurs in the material from Kjeller. From fig. 9 which demonstrates the diurnal rotation of the wind vectors, it is evident that the summer values indicate a complete rotation during the period 10^h—19^h, *i. e.* during nine hours.

A closer inspection of the wind-vector diagrams also indicates that the formal representation of the diurnal curve through Fourier-series must be viewed with caution. In the diagrams the rotation of the wind-vector has been drawn up with heavy lines during the part of the day when normal *E*-echoes can be recorded. It is evident that during day-time condition the rotation of the wind-vector is fairly regular. From the monthly wind-vector diagrams published by Phillips[7], covering

the years 1949 and 1950, it is also seen that for a number of months the movement of the wind-vector during the day is more regular than during night-time conditions.

It is also seen that there is a tendencty to close the wind-vector curve during a time of about 12 hours. During *night-time* conditions, indicated by broken lines, the movement of the wind-vector curves is highly irregular, but during all four seasons there is a tendency to turn over to a strong *westerly* drift during night time conditions when *E*s-echoes have been recorded.

The effect of the night-time conditions on the wind is easily seen from fig. 4 *a*, *b*, *c* and *d* on which the diurnal curves for the critical frequencies of *E* have been drawn at the bottom of each monthly plot. There is a sudden change in direction of the W—E conponent in the morning, and in the afternoon at about the time when the critical frecuency of the normal *E*-layer crosses the test frequency, 2 Mc/s. This means that the average drift

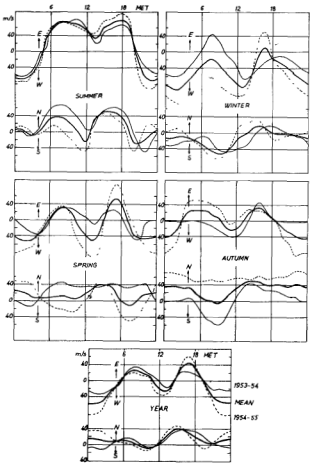

Fig. 6. Mean seasonal curves for the two years.

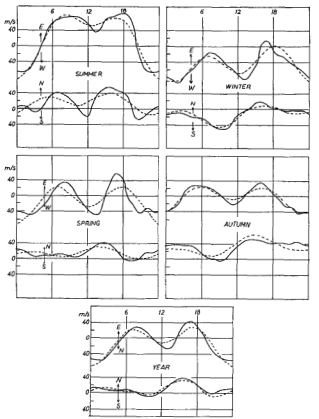

Fig. 7. Mean seasonal curves, full lines, compared with three term Fourier-synthesis, broken lines.

determined from *E*s-echoes during *night* conditions shows a strong increase of the *westerly* component.

Table 4 shows the coincidence between the time of normal *E*-echoes coming in the morning or disappearing in the afternoon, and the change-over in the E—W component from an *E*- to *W*-value.

Table 4.

	Normal *E*-echoes *in*	Change in E—W compo-nent	Normal *E*-echoes *out*	Change in E–W compo-nent
	MET	*MET*	*MET*	*MET*
June 1953....	5.30	5.30	19.40	18.30
Oct. — ...	8.40	9.30		
May 1954 ...	5.40	6.0	18.30	18.0
June — ...	5.20	5.0	19.20	19.0
July — ...	5 30	6.30	19.0	19.0
Nov. — ...	10.20	10.0		
March 1955 ...	8.0	8.0	16.30	16.30
June — ...	5.0	5.0	19.30	19.30
July — ...	5.10	6.0	19.30	19.30

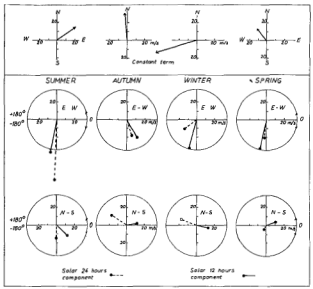

Fig. 8. Seasonal variation of the three terms in the Fourier series.

It is difficult to separate quantitatively these two effects of the normal E and Es in the diurnal trend with any accuracy, however, we may indicate the idealized windvector diagrams during the four seasons qualitatively, as shown in fig. 10.

The change-over in the E—W component after sunset may be ascribed to two effects; *a* a systematic change in height when going from normal E- to night Es-reflections and *b* to an anisotropy in the diffraction pattern with a preferred N—S direction. This question will be discussed in Section 10 of this paper.

We have here assumed that the 12-hours component due to the normal E-echoes, which is only apparent during the day, is also maintained during following 12 night hours. The strong westerly wind-component which occurs when Es-echoes are recorded appears superimposed on this during the night.

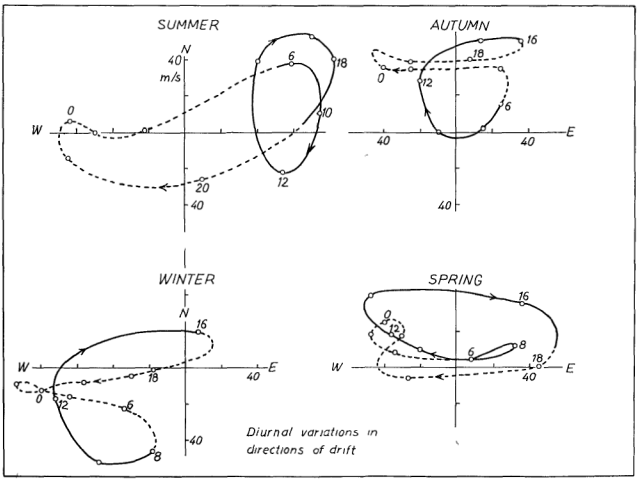

Fig 9. Windvector diagrams during the four seasons. The full lines indicate day conditions with normal E + Es reflections, the broken lines indicate night conditions when only Es-echoes have been present.

The question as to whether the solar 12-hours component is maintained continously during two complete revolutions during twentyfour hours, can only be settled from investigations at a place where the normal *E*-layer is present with sufficient density during night. It is planned to record *E*-wind at Tromsö (70° N) during The International Geophysical Year 1957—58, and during the months June and July the density of the normal *E*-layer should here be sufficient to give normal *E*-echoes on 2 Mc/s even during night hours.

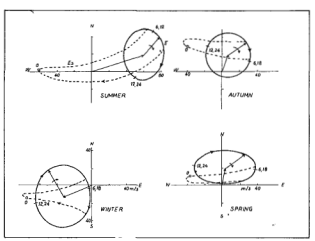

Fig. 10. Schematic wind-vector diagrams during the four seasons. The full lines indicate the rotation of the wind-vector when the normal *E*-layer is present. The broken lines indicate wind directions recorded during night conditions when only *Es* have been present.

It is previously stated from measurements in Cambridge that the normal *E*- and the *Es*-echoes *during the day* seem to give the same drift velocities of the diffraction pattern. During the summer season we have separated the days with normal *E*- and *Es*-echoes for a number of months and we find that both types of echoes indicate the same main character of drift. On fig. 11 is shown the diagram for Aug. 1954, the dots indicating values from normal *E*-echoes the circles from *Es*-echoes. The character of the E-echoes were estimated from the P', f-curves taken from routine observations at the nearest half hour.

In the E—W component there is a tendency to increase the number of westerly values during *Es* and in the N—S component there is a slight tendency to increase the number of southerly values during *Es*, effects which we have also noticed during other months.

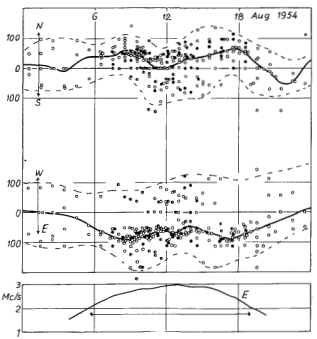

Fig. 11. Drift measurements Aug. 1954. The dots indicate values obtained from normal *E*-echoes, the circles from *Es*-echoes.

Lunar-time Variations.

In order to test the existance of a lunar component the hourly values have to be grouped according to lunar time. At Kjeller the summer months show the most regular diurnal variation, and in the analysis of the lunar component we have therefore only used the summer registrations. The following periods have been used: May to August 1954 and June to July 1955. For 1954 we have used the hourly values obtained during the whole 24 hours, for 1955 the values recorded during 5^h—19^hMET period.

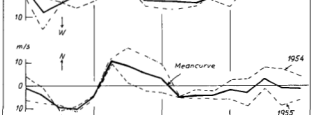

Fig. 12. Lunar day variations.

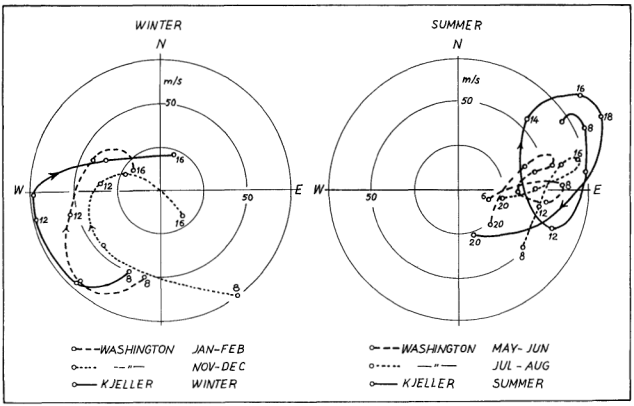

Fig 13. Wind-vector diagrams for Kjeller and Washington.

Fig. 12 shows the results of the mean variations during the lunar day.

There is an indication of two daily maxima in the curves. A Fourier analysis gave the following values:

$\triangle E = 0{,}6 \sin(\tau + 99°) + 4{,}3 \sin(2\tau + 159°)$ m/s

$\triangle N = 3.4 \sin(\tau + 244°) + 6.5 \sin(2\tau + 124°)$ »

The lunar wave is very small and it may be doubted whether the effect is real.

4. Comparison with other series of observations.

Series of observations of some lengths which have given curves showing the diurnal and annual variations have been made at Cambridge[9], Ottawa[10] and Washington[11] and it is of interest to compare these results with the Kjeller series.

a *Solar 12-hours term.*

According to Gautier[12] the Washington records now extend over a period of three years. Detailed numerical results have not yet been published, the wind-vector diagrams have been made available. It is of interest to compare the summer and winter wind-vector diagrams during day-time for Kjeller and Washington, see fig. 13.

During winter time there is a close similarity between the Washington and Kjeller diagrams both in shape and magnitude. During summer time however, the Kjeller diagram shows a clear and predominant 12-hours rotation, whereas the Washington diagram shows a complex structure. During both seasons the wind vectors are in the same quadrant.

Briggs and Spencer[9] have given a survey of the Cambridge recordings up to 1954. The most striking feature is here a strong solar 12-hours component. In fig. 14 the solar 12-hours component from Cambridge has been drawn up in order to compare this with the Kjeller values. There is a qualitative agreement between Cambridge and Kjeller concerning the seasonal variation of the 12-hours solar component, and in Table 5 the values of solar 12-hours term from the Fourier analysis have been compared.

It should be emphasized that the summer values must be considered as more reliable than the curves for the other seasons. Concerning the mean annual curve there is an almost complete agreement between Cambridge and Kjeller.

Table 5. Solar 12-hours component, m/s.

	Cambridge 1949—53	Kjeller Jun. 1953—Sep. 1955
	N—S	N—S
Winter ...	40 sin(2t + 57°)	14 sin(2t — 7°)
Spring....	30 sin(2t — 30°)	11 sin(2t + 20°)
Summer ..	6 sin(2t — 66°)	18 sin(2t — 45°)
Autumn ..	16 sin(2t + 30°)	12 sin(2t + 11°)
Mean.....	14 sin(2t — 12°)	12 sin(2t — 14°)
	E—W	E—W
Winter ...	45 sin(2t — 78°)	33 sin(2t — 106
Spring....	39 sin(2t — 120°)	33 sin(2t — 104°)
Summer ..	20 sin(2t — 123°)	38 sin(2t — 103°)
Autumn ..	6 sin(2t — 42°)	23 sin(2t — 59°)
Mean.....	21 sin(2t — 93°)	31 sin(2t — 97°)

For Ottawa Chapman[10] gives the following mean values for the period Now 1950 — June 1951 of the solar 12-hours component:

$$\triangle E = 23 \sin(2t - 87°), \quad \triangle N = 34 \sin(2t - 10°)$$

The E—W component at Ottawa is thus in complete agreement with Cambridge and Kjeller, whereas there is an almost 90° phase difference in the N—S component.

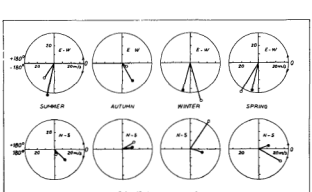

Fig. 14 Solar 12-hours component at Kjeller and Cambridge.

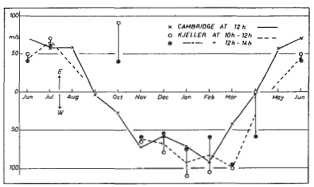

Fig. 15. Noon values of drift of the E—W component at Kjeller and Cambridge.

b *Solar 24-hours component.*

Concerning the solar 24-hours component no numerical data have been published from Cambridge and Washington.

c *Constant term.*

The wind-vector diagrams from Washington indicate during the day a S—W component in winter and a N—E component in summer, in close agreement with the constant term at Kjeller. According to the survey given by Ratcliffe[13] the same mean drift directions appear in Cambridge. Briggs and Spencer have given the mean monthly values of the E—W component at 12*h* for Cambridge, and the noon values at Kjeller show a similar annual variation, see fig. 15.

d *Lunar 12-hours term.*

The Kjeller records from the summers 1954 and 1955 show only a very small lunar 12-hours amplitude, the magnitudes and phases of which we regard as doubtful. In the following Table 6 the Kjeller values are compared with the survey given by Briggs and Spencer[9]

The Kjeller and Cambridge series of summer values, which are the most complete and reliable, have been used for the analysis. At both places the summer values indicate a very small component which must be regarded as doubtful. Series extending over the whole year however, as used by Chapman and Spencer, bring out a component of a magnitude which is comparable with the solar 12-hours term.

The conclusion from the discussion above, is that the existence of a lunar term in the summer values at Kjeller must be small and of a size not comparable with the solar 12-hours term.

Table 6. Lunar 12-hours component.

	N—S	E—W	
	Doubtful	Doubtful	
Kjeller	6 sin(2τ + 124°)	4 sin(2τ + 159°)	Harang summer 1954,55
Ottawa ...	24 sin(2τ + 3°)	21 sin(2τ + 106°)	Chapman. 1950—51
Washington	not detectable		
Cambridge	14 sin(2τ + 4°)	16 sin(2τ − 81°)	Phillips. 1949—51
—	not detectable		
—	Doubtful	Doubtfull	
	14 sin(2τ + 125°)	12 sin(2τ − 20°)	Spencer. Sep. 1952.

5.0 THE PERIOD OF FADING

From a number of records taken by optical method the total time of duration of ten fadings were measured and a figure expressing the mean duration of one fading. T_f, as computed. The dependence of T_f on the geomagnetic activity, measured through the K-index and on the total drift velocity V was investigated.

a. *Variation with geomagnetic activity.*

In the range of geomagnetic activity represented by K lying between 0 and 4, there seemed to be no systematic variation in V with a systematic increase in K. During periods of strong geomagnetic storms however we have a number of examples of very rapid fading with simultaneous high values of drift velocity. The record reproduced in fig. 2 *d* is an example of this effect. Similar striking effects have been reported by Phillips[7] A moderate storm however, does not seem to have any marked influence on the period of fading.

The K-values here used were taken from the records at the Auroral Observatory at Tromsö, and they thus represent the activity in the vicinity of the Auroral zone, which is lying about 11° farther North.

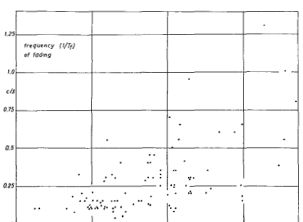

Fig. 16. Variation of fading frequency, $1/T_f$, with total drift velocity, V.

b. *Variation with total drift velocity, V.*

In fig. 16 we have compared the fading frequency, $1/T_f$, with the drift velocity V for the months Oct.—Nov. 1953 and Jan.—Apr. 1954.

There is a gradual increase in the fading frequency with velocity, and we note especially that values of V greater than 100 m/s appear only when the fading frequency has a value greater than 0,5 c/s.

6.0 EFFECT OF POLARIZATION

In the first paper on systematic drift measurements, Mitra[3] pointed out that «artifical» drift effects could occur if open antennas were used, either wires or frames, having different orientation. In the reflected echo both magneto-ionic components will be present having opposite rotation of their elliptic polarization. If the path difference between the two components changes gradually there will be a gradual rotation of the combined electric vector, and the open aerial will record a

periodic fluctuating voltage. Mitra demonstrated this effect on records taken with two open aerials, and stressed the importance of using polarized aerials which could receive only one component.

At Kjeller we have used only open aerials, either *L*-antennas or frames, with their planes lying in N—S direction. During day time the intensity of the extraordinary component on 2 Mc/s will be so weak that it will not have any disturbing influence. During nighttime however, both components may appear with appreciable intensity, and we should expect polarization effects on records. In fig. 17 are shown records with «polarization fading». In *a* both components have been of almost the same intensity, in *b* the amplitudes are different.

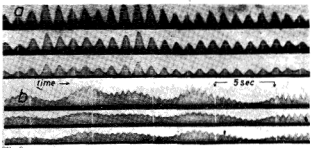

Fig. 17. Fadings on 2 Mc/s recorded on open *L*-aerials at three receiving points showing polarization effect. In *a* the ordinary and extraordinary component have been of the same magnitude, in *b* the amplitude of one component is considerably less than the other.

There is no noticable time difference between the maxima due to the fact that the directions of the open aerials have been parallel. On the Phillips records the effect of polarization fading should therefore either not be expected to appear, or, to appear as series of very small pips indicating an extremely high value of the drift velocity. In the interpretation of the records we have been aware of this possibility.

7.0 SHORT TIME VARIATIONS IN DRIFT DIRECTION

When the diurnal curves of drift are plotted for a series of consequtive days, one notices that the mean direction of drift in both components may change irregularly from one hour to the next even during daytime. During several months we have made simultaneous registrations of the mean echo *amplitude* of the E-echoes and also of the virtual *heights*, in order to see if the sudden changes in drift directions were associated with intensity variations, or with changes in virtual heights.

7.1 Intensity Effects.

From one of the receivers the *AVC*-voltage was applied to the third pen of the three-pen recorder, the two other pens recording the «spikes» giving the N—S and E—W drift components. An inspection of the records taken during a period of two months, showed no coincidence between deep fadings and changes in the drift directions.

7.2 Height Effects.

The height of the echoes, determined from P't-records was recorded through a separate *CRT* on photographic paper having a speed approximately of the same as the Phillips-records. Short periodic occurance of *Es* below the normal *E* was compared with the changes in drift direction. On individual days we have a number of examples showing a change in the drift when an *Es*-layer appeared for a short time.

a. *Observations on 11/10 1954. 10—16 MET.*

Normal *E*-echoes appeared around noon. The virtual height of the *E*-layer was recorded to 133—138 km, this high value being due to group retardation, as the critical frequency of the *E*-layer was only about 0.5 Mc/s above the test frequency 2 Mc/s. During 12.30—13.40 and *Es*-layer suddenly appeared at an height of 112 km.

The Phillips recorder during *Es*-layer showed great «spikes» giving the following values of the drift: $V_x = 38\ m/s$ towards W and $V_y = 30\ m/s$ towards *N*. The normal *E*-echoes before and after the *Es*-appearance gave the same unusually high value $V_x = 240\ m/s$ towards *E* and $V_y = 204\ m/s$ towards *N*.

b. *Observations on 21/12 1954. 10.30—11.30.*

On this day the critical frequency of the normal *E*-layer was below 2 *Mc/s*, and we obtained from an *Es*-layer in the height of 140—150 km. During

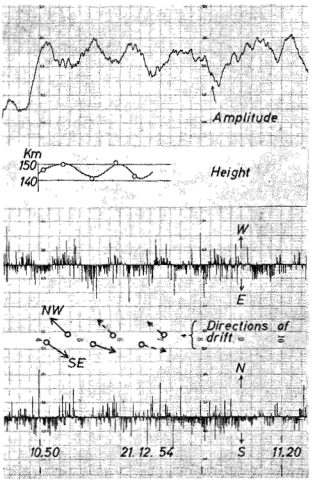

Fig. 18., Simultaneous recordings of amplitude, height and drift of an *Es*-layer, shows a periodic variation in amplitude and height accompanied by a periodic reversal of the drift direction.

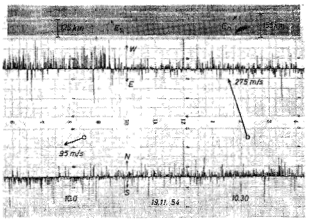

Fig. 19. Change in direction of drift when a new layer at a greater height is formed.

the time of recording the height of the layer changed periodically, and there was a parallel variation in the amplitude. During these oscillations the direction of drift changed periodically almost 180° from towards *SE* to *NW*.

c. *Observations on 19/11 1954. 10.10—10.30.*

During this day we have an interesting change-over from *Es* to normal *E*. In the morning before about 10.10 an *Es*-layer at an height of 125 km was present, giving good records indicating a drift towards *SW*. Then the *Es* faded away, and a layer with a virtual height of 155 km appearded, which is interpreted as the normal

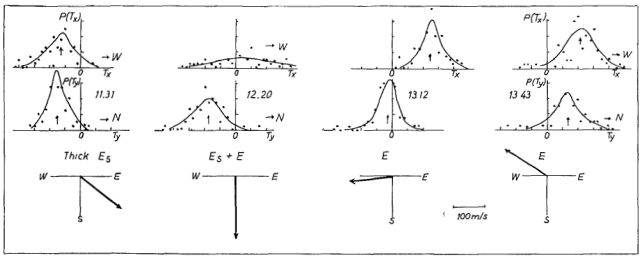

Fig. 20. Continous change of direction of the driftvector when the *E*-region changes from thick *Es* → *Es* + *E* → *E*.

E-layer coming in with considerable group retardation. The V_y component now changed from S to N and the wind-vector seemed to change about 90°.

7.3 Gradual Changes in Direction of Drift.

In the preceeding section a number of examples have been given which indicate sudden and discontinous changes in the direction of drift. On records from a single and stable E-layer we also may observe sudden changes in the drift, but we have also a number of cases in which a *continous* rotation of the wind-vector appears during a relatively short time. In the following some examples of this type of variation will be given.

a. *Records on 29/10 1954. 11.30—13.20.*

Strong echoes which gave reliable records from 9^h—15^h. From the routine $P'f$-records it was evident that the layer changed during the period of observations from a thick Es-layer, to $Es + E$ to E. As the Es-layer gradually faded out from the E-layer and the normal E remained, there was a continous rotation of the drift-vector, as seen from fig. 20. In the figure the distributions $P(T_x)$ and $P(T_y)$ of amplitudes on the Phillips record have been drawn up in order to determine the values of the mean time-displacements, T_x and T_y.

A similar effect appears on the records taken during the solar Eclipse on June 30th 1954, and will be discussed in connection with the eclipse observations.

8.0 MEASUREMENT OF DRIFT FROM SECOND ORDER ECHOES

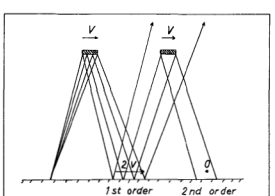

Fig. 21. The drift of the pattern on the ground in first and second order reflection when the waves are assumed to be reflected from a series of plane mirrors.

A discussion of the drift effects of the ionosphere on the *second order* echoes ground-pattern will illustrate the difference between the two models for the reflection process: the idealized models of a continous *refraction* process in a smooth ionosphere, and a *diffraction* process of the waves in an ionosphere containing irregularities. In the first case we will have as model the reflection of waves from a plane mirror, in the second case we will have diffractive reflection from a ground glass plate.

If we assume specular reflection the drift of a section of the pattern on the ground will be as illustrated in fig. 21.

A series of plane mirrors moving horizontally with a velocity V are reflecting the wave and we obtain a series of patches on the ground moving with a velocity $2V$. When the energy from these moving patches is again reflected from a suitable mirror, which now will have only the half of the velocity relative to the beam from the patch,

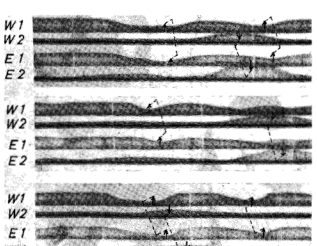

Fig. 22. Fading records taken over the W—E base on 1st and 2nd order E-echoes W1 and E1 are 1st order echoes recorded at the W and E receiving points. W2 and E2 are 2nd order echoes The corresponding maxima and minima are marked off, — there is no systematic difference in the displacement of the fading maxima in the two orders of reflection.

the patch appearing on the ground as second order reflection will be stationary.[1] On a number of days when *E*-echoes appeared with sufficient intensity to be recorded as second order reflections the hypothesis discussed above was tested. Four receivers were used and the first and second order echoes were gated separately and displayed on a four-beam oscillograph, providing an opportunity for investigating effect along either the N—S or E—W base. The result was as follows: the relative displacement of the fading maxima was *the same* in the first and second order reflections.

This result can be explained if we instead of the model of specular reflection assume the model of *diffractive* reflection outlined by Ratcliffe[19]. According to this model the fadings are produced by the Doppler-effect of moving diffractng centres which are distributed at random. In this diffraction process the «pre-history» of the primary wave falling in on the radiating centres will be of minor importance as the fadings will be produced by separate diffraction process during the first and second reflection.

[1] The authors are indepted to Mr. F. Lied for pointing out this effect.

9.0 OBSERVATIONS DURING THE SOLAR ECLIPSE, JUNE 30TH, 1954

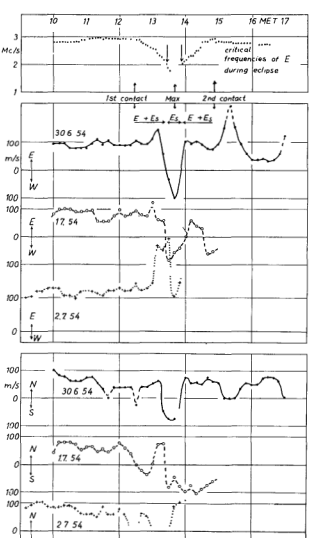

Fig. 23. Variations in the *E*-layer drift on the day of eclipse and the two following days.

E-layer drift records were taken during the day of the eclipse, and also on the two following days for comparison. At Kjeller the eclipse was 99.5 %, the first contact was at 12.26, maximum at 13.40 and the last contact at 14.51 *MET*. These are values at the Earth's surface, and must be modified for the height of the *E*-layer.

The records on these three days were of good quality, and values of the drift was determined for each ten minutes. Fig. 23 shows the variations of the drift in the E—W and N—S components.

The dotted curve at the top of the figure shows the variation in the critical frequency of normal *E* on the day of eclipse (after Landmark, Lied, Orhaug and Skribeland[14].

During the hours before noon the conditions were regular and similar on all three days, with a constant drift towards E and N. During the maximum period of the eclipse there is a symmetric dip in both the E—W and N—S components, and during the maximum of the eclipse the wind-vector has turned 180 ° from *NE* to *SW*.

However, the two following days show similar sudden changes during the same hours, and an unambigous interpretation on the dip during the solar eclipse as an eclipse effect appears doubtful. An inspection of the monthly curves for June and July in fig. 4 *a* to *d* shows that during the hours just after noon there is a considerable

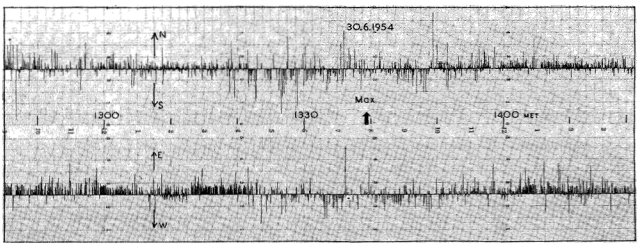

Fig. 24. Drift record during the eclipse. During the maximum period of the eclipse the direction of drift has changed from NE to SW.

spread in the values, and there appears a sudden change in the direction of the mean value of the N—S component.

In a recent paper, Landmark, Lied, Orhaug and Skribeland[14] have given the changes in electron densities of the layers at Kjeller during the eclipse, based on *P'f*-records, and the following characteristics of the *E*-layer region can be given. During the day of the eclipse there was a normal *E*-layer in which an *Es*-stratum was present. The electron density of normal *E* decreased during the eclipse, making an almost symmetrical dip, the *Es*, however, was present during the eclipse and was apparently not influenced by obscuration of the sun.

However at the moment when the critical frequency of the changing normal *E*-layer crosses the value of our test frequency, 2 *Mc/s*, a sudden change in the drift directions appears. From this moment we are obviously measuring only the *Es*-drift. The coincidence between the time of change in drift direction, and the change in the condition $Es + E \rightarrow Es \rightarrow Es + E$, indicates that the reversal of the drift has been an eclipse effect. The change in drift direction may be ascribed to an height difference between normal *E* and *Es*. Due to group retardation, it is difficult in this case to give estimates of the true geometrical heights of the reflecting layers.

10.0 THE STATISTICS OF TIME SHIFTS

10.1 Theory.

A strip of a Phillips-record gives an impression of the great variability of the time shifts. From a record of suitable length usually half an hour is sufficient, the number of deflections occuring within selected limits of amplitude can be counted, and the probability distributions $P(T_x)dT_x$ and $P(T_y)dT_y$, can be given as functions of T_x and T_y. These two curves form the experimental base for the analysis of the properties of the diffraction pattern.

The statistics of T_x and T_y has been treated in a series of papers by Briggs, Phillips and Shinn[5]. Briggs and Phillips[6], Briggs and Page[15] and Briggs and Spencer[16], and along slightly different lines by Ratcliffe[8] and Newstead[17]. In the following we shall apply the theory in the form developed by Briggs et al.

The theory has been discussed at the following three stages of increasing complexity of the diffraction pattern:

a. isotropic pattern which is drifting unchanged with constant velocity V,
b. isotropic pattern which is changing,
c. anisotropic pattern which is changing.

In the *first* case a system of formulas can be given which describes completely the probability

distributions $P(T_x)$ and $P(t_y)$. In the *second* case the effect of change of the pattern is measured as a quantity V_e which has the dimension of a velocity. It is not possible from the two distribution curves to derive explicite values of V and V_e, but by selecting suitable values of V and V_e, it is in some cases possible to obtain a close fit between observed and calculated distribution curves. In the *third* case, it is not possible from only two distribution curves, to derive the degree of anisotropy. Briggs and Spencer[16] have however shown, that if a third base is used simultaneously, it will be possible to detect an isotropy effect.

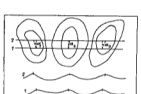

Fig. 25. Movement of a «twodimensional» random function. The differences in time-shifts are determined by $tg\alpha$, after Briggs and Page.

Briggs and Page[15] have made an empirical study of the following problem. The isotropic pattern with its contour lines is regarded as a «twodimensional» random function having certain values of autocorrelation function. A line is drawn, (representing for instance the E—W base), and it is evident that the maxima in the pattern will indicate the time shifts if the pattern is drifting in the direction of the line. A second and parallel line is drawn at a close distance δ. The drift of the pattern is in this case also given by the mean value of the time shifts, but there will be a difference in the position of the two time-shifts along the lines 1 and 2, which is determined by $tg\alpha$, and it is evident that $tg\alpha$ will have a certain probability distribution. It has not been possible to deduce this function explicity from the properties of the random functions, but Briggs and Page have shown that a probability function of the type

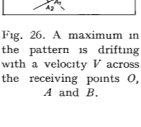

Fig. 26. A maximum in the pattern is drifting with a velocity V across the receiving points O, A and B.

$$\Phi(\mathrm{tg}\alpha) = C\exp(-\mathrm{tg}^2\alpha/0{,}74) \qquad (10.01)$$

is in accordance with results from numerical experiments with «two-dimensional» random functions having different values of autocorrelation functions.

In a second paper Briggs and Spencer have applied this probability function in their discussion of probability distributions of T_x and T_y. From fig. 24 we obtain:

$$T_x = A\,A_1/V, T_y = B\,B_1/V, \text{ and further} \qquad (10.02)$$

$$\begin{aligned} T_x &= \xi_o\cos\varphi/V - A_1A_2/V, \\ T_y &= \eta_o\sin\varphi/V + B_1B_2/V \end{aligned} \qquad (10.03)$$

The mean values, $\overline{T}_x$ and $\overline{T}_y$, will be:

$$\overline{T}_x = \xi_o\cos\varphi/\mathrm{V}\,,\ \overline{T}_y = \eta_o\sin\varphi/\mathrm{V} \qquad (10.04)$$

The probability of observing T_x within a range T_x to $T_x + dT_x$ is given by the function $P(T_x)dT_x$, and it is evident that this function must be related to the probability function $\Phi(\mathrm{tg}\alpha)$. We have now:

$$A_1A_2 = OA_2\mathrm{tg}\alpha = \xi_o\sin\varphi\mathrm{tg} \qquad (10.05)$$

From (10.05) and (10.03) we obtain:

$$\mathrm{tg}\varphi = (VT_x - \xi_o\cos\varphi)/\xi_o\sin\varphi \qquad (10.06)$$

giving:

$$\begin{aligned} \Phi(\mathrm{tg}\alpha)d\alpha &= \Phi\left[\frac{VT_x - \xi\cos\varphi}{\xi_o\sin\varphi}\right]\frac{V}{\xi_o\sin\varphi}\,dT_x \\ &= P(T_x)dT_x \end{aligned} \qquad (10.07)$$

By using (10.04) we further obtain:

$$\begin{aligned} P(T_x) &\propto \Phi\left[\frac{V(T_x - \overline{T}_x)}{\xi_o\sin\varphi}\right] \\ &= \Phi\left[(T_x - \overline{T}_x)/(\xi_o^2/V^2 - \overline{T}_x^2)^{\frac{1}{2}}\right] \end{aligned} \qquad (10.08\,\mathrm{a})$$

and similarly:

$$\begin{aligned} P(T_y) &\propto \Phi\left[\frac{V(T_y - \overline{T}_y)}{\eta_o\cos\varphi}\right] \\ &= \Phi\left[(T_y - \overline{T}_y)/(\eta_o^2/V^2 - \overline{T}_y^2)^{\frac{1}{2}}\right] \end{aligned} \qquad (10.08\,\mathrm{b})$$

If we have $\xi_o = \eta_o = a$, we have that the widths of the distribution curves will be proportional respectively to $a\sin\varphi/V$ and $a\cos\varphi/V$, see fig. 25 *a*, and we obtain the following result which can be tested experimentally:

$$\text{width of } P(T_x)/\text{width of } P(T_y) = \mathrm{tg}\varphi = \overline{T}_y/\overline{T}_x \qquad (10.09)$$

In some of the Kjeller records the time scale has been sufficiently open to be able to determine corresponding values of T_x and T_y. In this case it will be possible to plot corresponding values of T_x and T_y in a (T_x, T_y) — plane, and it is easy to show that for an unchanging pattern the

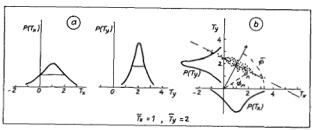

Fig. 27. Probality curves of T_x and T_y. *a*) — separate, *b*) — in a (T_x, T_y) — plane.

points in the (T_x, T_y) — plane lie on a straight line. From fig. 24 we obtain:

$$B_1B_2 = A_1A_2\text{cotg}\varphi \text{ (when } \xi_o = \eta_o), \quad (10.10)$$

introducing this in (10.03) and eliminating A_1A_2 we obtain:

$$T_x - T_x + \text{tg}\varphi(T_y - T_y) = 0 \quad (10.11)$$

Where $\text{tg}\bar{\varphi} = \bar{T}_y/\bar{T}_x$.

Instead of the equation (10.11) we may also use the following equation for the line:

$$T_x\bar{T}_x + T_y\bar{T}_y = \bar{T}^2 \quad (10.12)$$

where $\bar{T}^2 = \bar{T}_x^2 + \bar{T}_y^2$.

It is obvious that this line is at right angle to the mean direction of the drift (determined by $\text{tg}\bar{\varphi} = \bar{T}_y/\bar{T}_x$).

The probability distribution of T_x and T_y will therefore be as indicated in fig. 27 *a* and *b*[1].

As mentioned by Briggs and Spencer, it is often observed that the component with the greatest time shift shows the narrowest distribution curve which should indicate that the pattern was moving unchanged with constant velocity. As a second criterion the points in the (T_x, T_y) — plane should in this case give a straight line.

10.2 Observations.

In addition to the time-shift measurements along the E—W and N—S bases, it was also possible to measure the timeshift along the W—S diagonal base on the three-pen recorder, The time-shifts along the diagonal base will be equal to the algebraic sum of the time-shifts along the other main bases.

In the following, a number of cases will be treated in which the direction of drift has been especially simple: either *diagonal* to the main bases or *along* one of the main base-lines.

a) *Drift diagonal to the base-lines.*

It is evident that in this case the time-shift along NW— or *SE*-directions should be twice the time-shifts along E—W or N—S bases. Table 7 and fig. 29 give the results from three strips of records taken about noon.

Table 7.

		Time-shifts			Widths		
		$\bar{T}_x$	$\bar{T}_y$	$\bar{T}_d$	E—W	N—S	Diag.
16 2.1955.	12.16	2.6 W	2.7 N	7 5 NW	2.7	2.7	7 0
17.2.1955.	13.06	2.5 E	2.5 S	5.4 SE	4.4	3.0	8.7
18.2.1955.	12.12	3.9 W	5.5 N	11.3 NW	4.7	4.1	8.0
	Mean	3.0	3.6	8.1	3.9	3.3	7.9

From Table 7 the following two effects are evident:

i. the mean value of *time-shifts* T_D and the width of the distribution curve along the diagonal is approximately equal to the sum of the time shifts and widths along the main base lines. This is in accordance with the theory for a changing, but isotropic pattern.

ii. the *width* of the distribution curve in E—W is in all three cases *greater* than in N—S. This

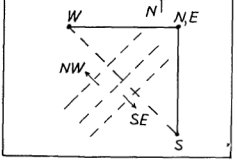

Fig. 28. Direction of drift, a) diagonal to the main base-lines, b) along one of the base-lines.

[1]) In a recent paper of Court[18] a method for analyzing wind records is discussed which is similar to the discussion above. By plotting the(T_x, T_y) — values in a plane the line according to equation (10.11) or (10.12) is drawn and — as shown in Fig 27 — the angle $\bar{\varphi}$ and the value of $\bar{T}$ can be determined. Court has however not considered the complete and random distribution of the "lines of maxima".

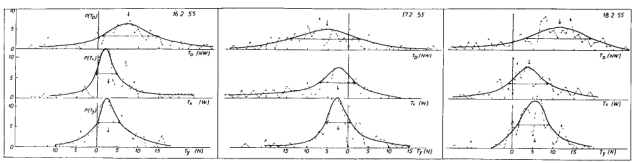

Fig. 29. Distribution curves in $P(T_x)$. $P(T_y)$ and $P(T_D)$.

is *not* in accordance with the assumption of an isotropic pattern. In the following additional examples of this effect will be given.

b) *Drift direction along one of the base-lines.*

In this case the mean value of time-shift along one of the base-lines is zero, for the other base-line and along the diagonal the mean values of time-shifts are equal. In fig. 30 a series of six records taken at noon in Jan—.Febr. have been analyzed, the length of the record being twelve minutes. In all cases the mean value of time-shift in N—S direction was nearly zero, and along the E—W base there was a drift towards West. The mean values of time-shifts and widths are given in Table 8.

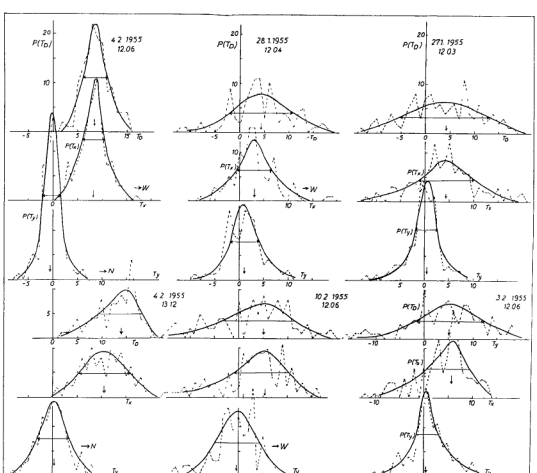

Fig. 30. Distribution curves in $P(T_x)$. $P(T_y)$ and $P(T_{Diag.})$

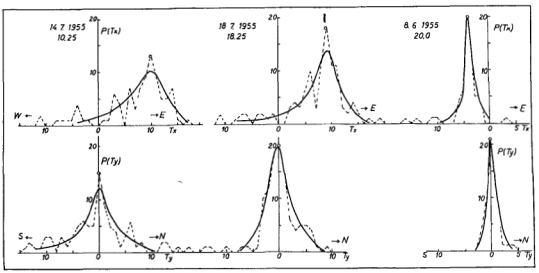

Fig. 31. Distribution curves with decreasing widths.

Table 8.

Date	Time-shift			Width		
	T_x	T_y	T_D	E–W	N–S	Diag.
4 2.1955...	8,2 W	0.6 S	8.4	4 6	3.8	5.4
28.1. -	3.0 W	1.0 N	4.2	7.2	6.2	13.0
27.1. -	4.3 W	0.4 N	4.3	11.6	4.8	18.8
4.2. -	10.6 W	0.4 N	14.0	10.7	6.5	8.5
10.2. -	5.4 W	0.4 S	5.1	11.5	9.4	15.0
3.2. - ..	5.8 W	0.5 N	5 2	7.9	4.6	14.4
Mean:	6.2 W	0.2 N	6 9	7.9	5.9	12.5

From Table 8 it is evident that the mean value of time-shift along the E—W base coincides with the time-shift along the diagonal-base. The length of the diagonal base is in this case equal to $\sqrt{2}$(E—W), and the increase in length of the diagonal base will decrease the correlation of the two fading curves, giving a considerably greater width of the $P(T_D)$-curves. Also here we notice a greater width of the distribution curve along the E—W base than along the N—S base, the latter having zero time-shifts. This effect is not in agreement with the assumption of an isotropic pattern. The different widths of the distribution curves in N—S and E—W directions indicate that the «lines of maxima» in the diffraction pattern have considerably smaller variability around the N—S direction, than around the E—W direction. If we assume that the pattern, instead of being isotropic, consists of elongated «ridges», with a preferred orientation in N—S direction, the effect of different widths of the distribution curves can at least be explained qualitatively.

Probability-distribution Curves during the Night.

The type of distribution curves given in fig. 30 are characteristic of day time conditions. However during the night, we have a number of cases in which the distribution curves have been very

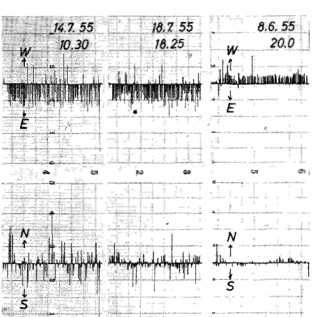

Fig. 32. Records of E—W drifts showing different «widths of distribution».

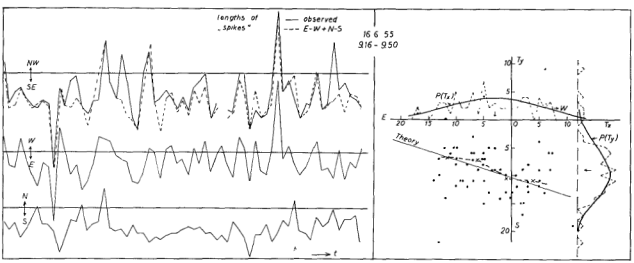

Fig. 33 a) The lenghts of the «spikes» on the diagonal, E—W and N—S bases, The broken line indicates the sum-curve of the E—W and N—S «spikes».
b) The (T_x, T_y)-values presented in a plane, the median values are indicated by crosses.

narrow. The drift was in these cases always along the E—W base, and usually towards W. Fig. 31 shows a number of distribution curves with decreasing widths. The records are shown in fig. 32, the first two curves representing day-time conditions. The very narrow curve recorded at 20^h represents the extreme case of a uniform drift towards W, with a strong preferred direction of the lines of maxima in the N—S direction.

It is evident that the high degree of anisotropy appearing on the third record in fig. 31 and 32 indicates that the «drift-velocity» towards W calculated in the usual way, may be entirely different from the actual drift of the diffraction pattern both in direction and magnetude. This effect may explain, at least partly, the irregular variation of the wind-vector during night, which is evident in fig. 9.

10.3 Presentation of the Time-shifts (T_x, T_y)-plane.

In fig. 27 *b* it is demonstrated that for an isotropic unchanged pattern the points (Tx, Ty) are expected to lie in a straight line determined by equation (10.11).

A number of records of great speed showing the «spikes» appearing simultaneously over the N—S. E—W and diagonal bases have been obtained, and in fig. 33 an example of analysis has been given. As previously mentioned the «spikes» appearing on the diagonal base shall be the sum of the «spikes» recorded on the two other bases. On the upper line the sum curve is drawn up as a broken line, which is to be compared with the continous line representing the «spikes» recorded. The parallel trend of the two curves indicates that the recording equipment has been working properly. The distribution of the points in the (T_x, T_y)-plane is considerably more scattered than expected, even when due allowance is made for the limited accuracy. However the positions of the median values of the points — indicated by crosses — lie on the expected theoretical line.

REFERENCES

[1] STÖRMER, C.: Astrophysica Norvegica. *1*. No. 3 (1935) and *3*. No. 5 (1939).

[2] LILLER, W., and F. L. WHIPPLE: See article in: Rocket Exploration of the upper Atmosphere. 112 (London 1954).

[3] MITRA, S. N.: P. I. E. E. Pt. III. *96*, (1949) 441.

[4] LIED, F.: F. F. I. Internal Report No. 34 (1950).

[5] BRIGGS, H. B., G. J. PHILLIPS, and D. H. SHINN: Proc. Phys. Soc. *63*. (1950). 106

[6] BRIGGS, B. H. and G. J. PHILLIPS. Proc. Phys. Soc. *63* (1950) 907.

[7] PHILLIPS, G. J.. Journ. Atm. Terr. Phys. *2* (1952) 141.

[8] RATCLIFFE, J. A.: Journ. Atm. Terr. Phys. *5* (1954) 173.

[9] BRIGGS, B. H., and M. SPENCER: Rep. on Progr. in Physics. (Phys. Soc.) *17* (1954) 245.

[10] CHAPMAN, H. J.: Canadian Journ. Phys. *31* (1953) 120.

[11] SALZBERG, C. D., and R. GREENSTONE. Journ. Geophys. Res, *56* (1951) 521.

[12] GAUTHER, T. N.: Scientific American *193* (1955) 126.

[13] The Physics of the Ionosphere Rep. of the Phys. Soc. Con. on the Physics of the Ionosphere. (London 1955.)

[14] LANDMARK, B. F. LIED, T. ORHAUG, and S. SKRIBELAND Geofys. Publ. *19* (1956) No. 8.

[15] BRIGGS, B. H., and E. S. PAGE. The Physics of the Ionosphere. Rep. of Phys. Soc. Conference (London 1955) 119.

[16] BRIGGS, B. H., and M. SPENCER: The Physics of the Ionosphere. Rep. of Phys. Soc. Conference (London 1955) 123.

[17] NEWSTEAD, G. Journ. Atm. Terr. Phys. *5* (1954) 182.

[18] COURT, G. W.: Journ. Atm. Terr. Phys. *7* (1955) 333.

[19] RATCLIFFE, J. A.: Nature *162* (1948) 9.